IEEE Access
Multidisciplinary ⋮ Rapid Review ⋮ Open Access Journal

Received July 13, 2018, accepted August 13, 2018, date of publication August 22, 2018, date of current version September 7, 2018.

Digital Object Identifier 10.1109/ACCESS.2018.2866170

Effects of Second-Order Matched Stochastic Resonance for Weak Signal Detection

HAITAO DONG, (Student Member, IEEE), HAIYAN WANG, XIAOHONG SHEN, (Member, IEEE), AND ZHE JIANG, (Member, IEEE)
Key Laboratory of Ocean Acoustics and Sensing, Ministry of Industry and Information Technology, Northwestern Polytechnical University, Xi'an 710072, China
School of Marine Science and Technology, Northwestern Polytechnical University, Xi'an 710072, China

Corresponding author: Haiyan Wang (hywang@nwpu.edu.cn)

This work was supported in part by the National Key Research and Development Program of China under Grant 2016YFC1400200 and in part by the National Natural Science Foundation of China under Grant 61571365, Grant 61571367, Grant 61671386, and Grant 61771401.

ABSTRACT Weak signal detection via stochastic resonance (SR) has attracted considerable attention in a wide range of research fields, especially under heavy background noise circumstances. In this paper, a second-order matched stochastic resonance (SMSR) method is proposed to further improve the signal-to-noise ratio of weak period signal. By selecting a proper damping factor in the regime of second-order parameter matched relationship, weak periodic signal, background noise, and nonlinear system can be matched in generating an enhanced output. The matched relationship is deduced in combining noise intensity optimization and signal frequency synchronization with duffing system in a mathematical way, and a normalized scale transformation is further carried out to make it accessible in detecting arbitrary high frequency signals. The numerical analysis and application verification are performed to confirm the validity and effectiveness of theoretical results, which indicate the proposed SMSR method is superior to the first-order parameter matched stochastic resonance in achieving a good band-pass filtering effect with a low-noise output as the driving frequency of received signal is not too small ($\geqslant$0.1 Hz). Thus, the proposed method is beneficial to practical engineering weak signal processing and anticipates to be a potential novel technique for ship radiated line-spectrum detection.

INDEX TERMS Stochastic resonance (SR), parameter matched relationship, duffing oscillator, signal-to-noise ratio improvement (SNRI), ship radiated line-spectrum detection.

I. INTRODUCTION

Stochastic resonance (SR) has been proven to be an effective approach for weak signal detection, especially under low signal-to-noise ratio (SNR) circumstances. Since proposed by Benzi *et al.* [1] in 1981, it has attracted considerable attentions in a wide range of research fields for its distinct merit that the energy of weak continuous signal can be enhanced by exploiting the noise energy, and therefore increase the signal-to-noise ratio (SNR) [1]–[6]. As the SNR is often directly linked to the performance of a detector as a tenet, it is then studied as a potential new technique for weak signal detection [7]–[15]. Early achievements are mainly focus on the enhancement of weak signal detection by adding suitable noise, while it might be a suitable option of adding appropriate noise with lower noise intensity, but restricted of how to remove noise for a high level, especially under low SNR region. Hence, rather than adjusting the input noise level, tuning signal structure and (or) system parameters might be more suitable for practical signal processing applications. Xu *et al.* [16] extended the concept of "SR" and proposed a parameter-induced stochastic resonance (PSR) by tuning system parameters instead of noise, which greatly promotes the development of stochastic resonance for practical applications as tuning system is more easier to be implemented in most cases. Nevertheless, the tuning approach can not address the problem in detection of high-frequency modulating signals subjected to high noise levels for the sake of adiabatic approximation in theory, which is crucial for engineering applications as the frequency of received signals generally varies from tens to thousands of Hertz and the background noise is generally unknown [17]–[22].

To ease the small parameter limitation of classical SR (both signal frequency and signal amplitude should be far less than one), several improvements have been achieved by modifying and optimizing strategies to address large parameter signals, such as scale normalized SR [17], re-scaling frequency

SR [18], adaptive step-changed SR [19], frequency-shift and re-scaling SR [20], and multiscale noise tuning [21], etc. These studies are realized by tuning signal structures and (or) system parameters to form a small parameter circumstance, while proper initial system parameters and tuning ranges are generally selected empirically in many publications to avoid the divergent of numerical method and high computational costs. This is a considerable problem which seems that it can be resolved by giving a certain mathematical guidance of system design for the desired optimal output. Related previous studies mainly focus on analyzing the influence of signal structure, noise type or system parameters to optimize the system output by tuning [22]–[30]. A parameter matched relationship in mathematical form with first-order damped bistable SR model (FMSR) has been given in our previous work, while the enhancement performance is limited, especially under heavy background noise [31]. From the perspective of achieving better performance, studies of SR with second-order duffing equation are verified superior to the first-order Langevin equation (LE) as it can be regarded as a secondary filtering and hence produces a cleaner filtered signal than first-order SR [25], [27], [32], [33]. Therefore, it would be a new attempt to consider a second-order SR model with parameter matched stochastic resonance in improving the SR based weak signal detection effect.

Motivated by the above analysis, this paper focuses on realizing the parameter matched stochastic resonance with second-order duffing system (SMSR), aiming to achieve better performance for weak signal detection. The matching framework of second-order stochastic resonance is given in a mathematical way, and a normalized scale transformation is utilized to make it available in detecting arbitrary high frequency signals. The main contributions of this paper are summarized as follows: 1) a parameter matched relationship for system potential parameters with duffing oscillator is given in mathematical form, which can be used directly for matched system initialization; 2) the tuning range of damping factor is given and verified as it is proportional to driving frequency for desired matched output, which can be used efficiently in determining the searching range and interval with low computational costs for different frequency band signals; 3) the proposed SMSR method could achieve a superior denoising performance that is quite beneficial to extract the periodic signal from the heavy background noise, which is expected to be extensively utilized in weak signal detection.

The rest of this paper is organized as follows. Section II provides relevant theoretical framework of the proposed SMSR method and introduces the weak signal processing strategy via SMSR. In Section III, the simulation analysis to evaluate the SMSR method is performed in comparison with the FMSR method. Application verification is conducted in section IV to validate the effectiveness and efficiency of the proposed method by analyzing a set of hydrophone received ship radiated acoustic data. Finally, concluding remarks are drawn in Section V.

II. SECOND-ORDER PARAMETER MATCHED STOCHASTIC RESONANCE WITH DUFFING OSCILLATOR

A. BASIC MODEL

To describe the phenomenon of SR, second-order Duffing-Holmes nonlinear differential equation is adopted as below,

$$\frac{d^2x}{dt^2} + \gamma\frac{dx}{dt} = -\frac{dV(x)}{dx} + s(t) + n(t) \tag{1}$$

where γ is damping factor. $s(t) = Acos(2\pi f_0\, t+\varphi)$ represents the input periodic signal, in which A, f_0 and φ are amplitude, driving frequency, and initial phase of the periodic signal, respectively. $n(t) = D\xi(t)$ with $\langle n(t), n(t+\tau)\rangle = 2D\delta(t)$ stands for the noise, where D is the noise intensity and $\xi(t)$ represents additive Gaussian white noise (AGWN) with zero mean and unit variance. $V(x)$ is a quartic double well potential as written below,

$$V(x) = -\frac{a}{2}x^2 + \frac{b}{4}x^4, \quad a, b > 0 \tag{2}$$

in which a and b are barrier parameters of bistable potential. Without external forcing, the system exhibits two stable stationary attraction at $\pm x_m = \pm\sqrt{a/b}$ separated by a potential barrier with amplitude $\Delta V = a^2/(4b)$ and an unstable one at $x_0 = 0$ as shown in Fig.1 (choose $a = b = 1$ for illustration).

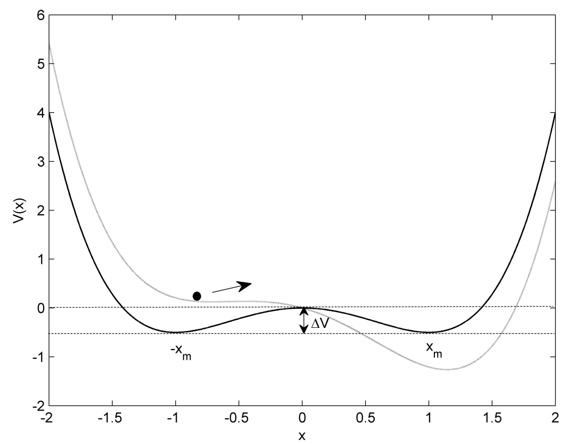

FIGURE 1. Bistable SR system potential $V(x)$ with periodical force modulation.

For a thorough understanding of the system behavior when forced by a stochastic signal, damping relaxation γ^{-1} and the characterization of particle oscillating inside the two potential wells must be taken into consideration. For this purpose, studies of Lyapunov's stability analysis have shown the nontrivial fixed points at $\pm x_m$ behave as desired stable focuses if the damping factor γ is restricted to the interval $0 < \gamma \leq 2\sqrt{2a}$, which gives us a constraint condition for parameter tuning [34]. Meanwhile, from the two-states theory, it is known in the presence of a periodic signal with suitable noise, if the mean passage time of particle between the two wells is equal to the half period of the driving periodic forcing applied to the particle, a statistical synchronization between noise induced transition and the weak periodic forcing occurs, and as a consequence, the SR phenomenon occurs [3]. The transition probabilities of particle coincide with Kramers rate r_K can be calculated as follows [3],

$$r_K = \frac{\omega_b \omega_0}{2\pi\gamma} \exp(-\frac{\Delta V}{D}) \tag{3}$$

where $\omega_b = [V''(\pm x_m)]^{\frac{1}{2}} = (2a)^{\frac{1}{2}}$ and $\omega_0 = [V''(x_0)]^{\frac{1}{2}} = (a)^{\frac{1}{2}}$ are the characteristic frequencies of system.

For the purpose of achieving the parameter matched relationship, it is initially considered that the Kramers rate r_K is the most important feature as the connection of signal, noise and system nonlinearity. Since signal-to-noise ratio improvemnet (SNRI) is mostly analyzed in SR theory, the principle of matched framework in this paper is on the basis of Kramers rate with SNRI maximization for desired enhancement performance.

B. MATCHED FRAMEWORK OF DUFFING OSCILLATOR

From the above analysis, we have a basic parameter condition for a matched SR system as $r_K = 2f_0$ within the regime of small parameter limitation. To the convenience of analysis, we could further define a discrimination function $F(a, b, \gamma, D, f_0)$ as below [26],

$$F(a, b, D, \gamma, f_0) = \frac{a}{2\sqrt{2}\pi\gamma f_0} exp(-\frac{a^2}{4bD}) \tag{4}$$

Obviously, the SR phenomenon occurs as $F = 1$, which is considered in connection with both driving signal frequency and noise intensity.

To achieve the desired optimal matched output, SNRI optimization is conducted. For sinusoidal signals with additive noise, the input SNR and the output SNR corresponding to equation (1) can be given as,

$$SNR_{input} = \frac{A^2}{4D} \tag{5}$$

and

$$SNR_{output} \approx \frac{aA^2\sqrt{2a}}{4bD^2} \exp(-\frac{a^2}{4bD}) \tag{6}$$

where the details of output SNR deduction for second-order system can be seen in [25]. Then we could have SNRI of duffing system as,

$$SNRI = \frac{SNR_{output}}{SNR_{input}} \approx \frac{a\sqrt{2a}}{bD} \exp(-\frac{a^2}{4bD}) \tag{7}$$

Intuitively, the SNRI is influenced by potential parameters and noise intensity. Hence, to achieve the desired output performance corresponding to noise intensity, optimization method can be utilized as,

$$D_{opt} = \underset{D}{\operatorname{argmax}}\ \text{SNRI}$$

By solving the first-order partial differential of equation (7) with respect to D, we have the optimal relationship between system parameters and noise intensity as,

$$D_{opt} = \frac{a^2}{4b} = \Delta V \tag{8}$$

Consider the detection problem with known frequency and initial phase in additive stationary noise, the signal frequency f_0 can be known as prior knowledge, and the noise intensity D would be thought of fixed in a certain period of time under high sampling frequency, which can be estimated by classical stochastic signal estimation methods. The parameter conditions for matched relationship then can be obtained in the satisfaction of,

$$\begin{cases} F = 1 \\ D = a^2/4b \end{cases} \tag{9}$$

C. LARGE PARAMETER MATCHING WITH NORMALIZED SCALE TRANSFORMATION

The matched framework of duffing oscillator in last subsection is given in the regime of small parameter limitation, while limited to be used for practical engineering fields. In order to match arbitrary high frequencies ($\gg 1Hz$), a normalized scale transformation is taken to form a small parameter circumstance.

Mathematically, let $z = x\sqrt{b/a}$ and $\tau = at$. Then equation (1) could be re-written as,

$$\frac{d^2z}{d\tau^2} + \frac{\gamma}{a}\frac{dz}{d\tau} = \frac{1}{a}z - \frac{1}{a}z^3 + \sqrt{\frac{b}{a^5}}Acos(\frac{2\pi f_0\tau}{a} + \varphi) + \sqrt{\frac{2bD}{a^5}}\xi(\frac{\tau}{a}) \tag{10}$$

In order to facilitate the expression, we introduce the variables substitution,

$$\frac{d^2z}{d\tau^2} + \gamma'\frac{dz}{d\tau} = a'z - b'z^3 + A'cos(2\pi f_0'\tau + \varphi) + D'\xi(\frac{\tau}{a}) \tag{11}$$

in which $\gamma' = \gamma/a$, $a' = b' = 1/a$, $f_0' = f_0/a$ $A' = \sqrt{b/a^5}A$, $D' = b/a^5 D$. By comparing equation (11) to equation (1), it is easy to find that the signal frequency is converted into $1/a$ times of the original signal frequency.

To the satisfaction of the SR matching principle required in the last subsection, substituting a', b', f_0' and D' into equation (9), we could have,

$$\begin{cases} F(a', b', D', f_0') = \dfrac{a'}{2\sqrt{2}\pi\gamma' f_0'} exp(-\dfrac{a'^2/4b'}{D'}) = 1 \\ D' = a'^2/4b' \end{cases} \tag{12}$$

With variables substitution, the matched parameter relationship of signal frequency, noise intensity and system parameters corresponding to equation (1) can be obtained as below,

$$\begin{cases} a = 2\sqrt{2}\pi f_0 \gamma e \\ b = a^4/4D \end{cases} \tag{13}$$

Intuitively, the damping parameter γ can be used for tuning the optimal matched output in the constraint condition of stable focuses as mentioned before. For desired stable focus of the nontrivial two stable stationary points, the damping factor γ' should be restricted to the interval of $(0, 2\sqrt{2a'}]$, and as a result,

$$0 < \gamma \leq 16\sqrt{2}\pi f_0 e \tag{14}$$

It can be seen that the stability interval of γ is proportional to driving frequency f_0, which means the optimal damping factor corresponding to the matched output for a higher driving frequency signal should be searched in a wider range and the stability of system output with higher driving frequency can be guaranteed more easily.

D. SIGNAL PROCESSING ALGORITHM VIA MATCHED OUTPUT TUNING

As indicated in the above subsection, the desired matched output with maximal SNRI can be obtained by tuning damping parameter γ in the framework of deduced matched relationship for a deterministic noisy signal. The corresponding flowchart is shown in Fig.2 and the detailed steps are summarized as follows:

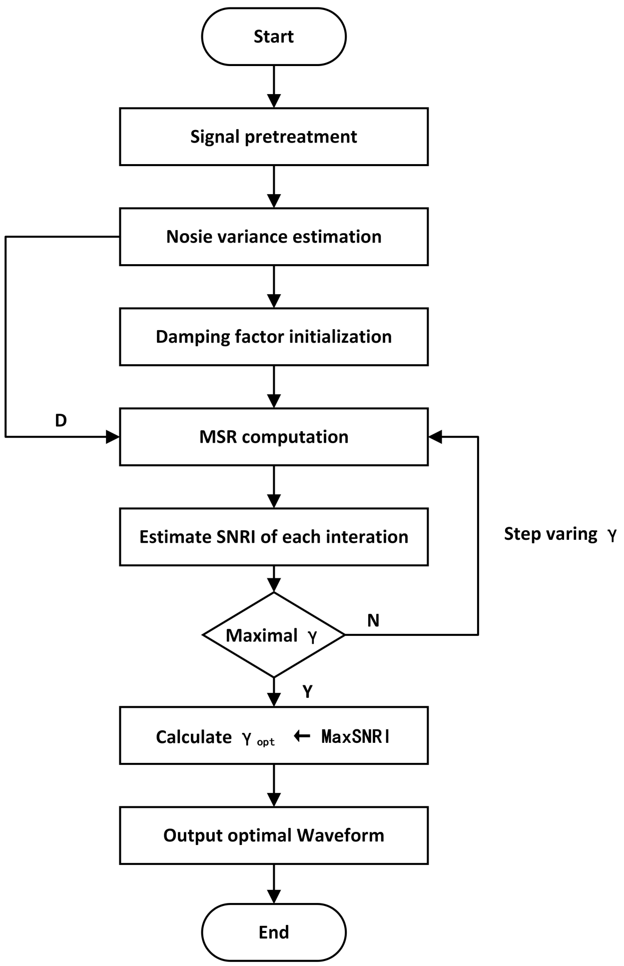

FIGURE 2. The algorithm flowchart of matched output tuning.

(1) Signal pretreatment. Common methods such as filtering or envelope extraction would be executed to better reveal the signal periodicity of actual received signals.

(2) Noise variance estimation. In this paper, the noise intensity can be estimated follow the principle of maximum likehood estimation (MLE) [35].

(3) Damping factor initialization. Initialize tuning range $[\gamma_{start}, \gamma_{end}]$ and tuning step γ_{step} of damping factor in accordance with the restriction of equation(14).

(4) MSR computation. The matched potential parameters a_{match} and b_{match} corresponding to the damping factor can be obtained via equation (13). Compute equation (1) to get output $x(t)$ by the Runge-Kutta algorithm, then estimate and store the SNRI.

(5) Tuning approach. Step varying the damping factor γ according to the initialized γ_{step} within the searching interval $[\gamma_{start}, \gamma_{end}]$ and repeat the process from step(4).

(6) Parameter Optimization. Calculate the optimal γ_{opt} corresponding to maximum SNRI according to the following objective function:

$$\gamma_{opt} = \underset{\gamma}{\operatorname{argmax}}\ SNRI$$

(7) Signal post-treatment. Output the waveform corresponding to highest SNRI value as the detected signal.

III. EFFECTS OF SMSR WITH COMPUTER SIMULATIONS

A. PERFORMANCE MEASURE WITH NUMERICAL METHOD

The above section provides the framework and implementation of second-order matched stochastic resonance. Alternatively, the fourth-order Runge-Kutta (RK4) method is employed to obtain the output sequence of SMSR [25],

$$\begin{cases} y_1 = y[n] \qquad y_2 = y[n] + x_1 h/2 \\ y_3 = y[n] + x_2 h/2 \quad y_4 = y[n] + x_3 h/2 \\ x_1 = -V'(x[n]) - \gamma y_1 + S[n] + N[n] \\ x_2 = -V'(x[n] + y_1 h/2) - \gamma y_2 + S[n] + N[n] \\ x_3 = -V'(x[n] + y_2 h/2) - \gamma y_3 + S[n] + N[n] \\ x_4 = -V'(x[n] + y_3 h/2) - \gamma y_4 + S[n] + N[n] \\ x_{n+1} = x_n + (y_1 + 2y_2 + 2y_3 + y4)h/6 \\ y_{n+1} = y_n + (x_1 + 2x_2 + 2x_3 + x4)h/6 \end{cases} \tag{15}$$

where h is the calculation step that is generally equal to $1/f_s$.

Here, typical measurement index of SNRI is adopted to discuss the effect of SR phenomenon for enhancing the energy of weak period signal by exploiting the noise component. Generally, the discrete time series of input and output power spectrum can be calculated via discrete Fourier transform (DFT) for engineering digital signal processing as,

$$SNR = 10\log_{10} \frac{A_f}{\sum_{i=1}^{N/2} A_i - A_f} \tag{16}$$

in which N is the length of the time series, A_f represents the power of driving frequency f_0, and the item $\sum_{i=1}^{N/2} A_i - A_f$ is the total power of noise [25].

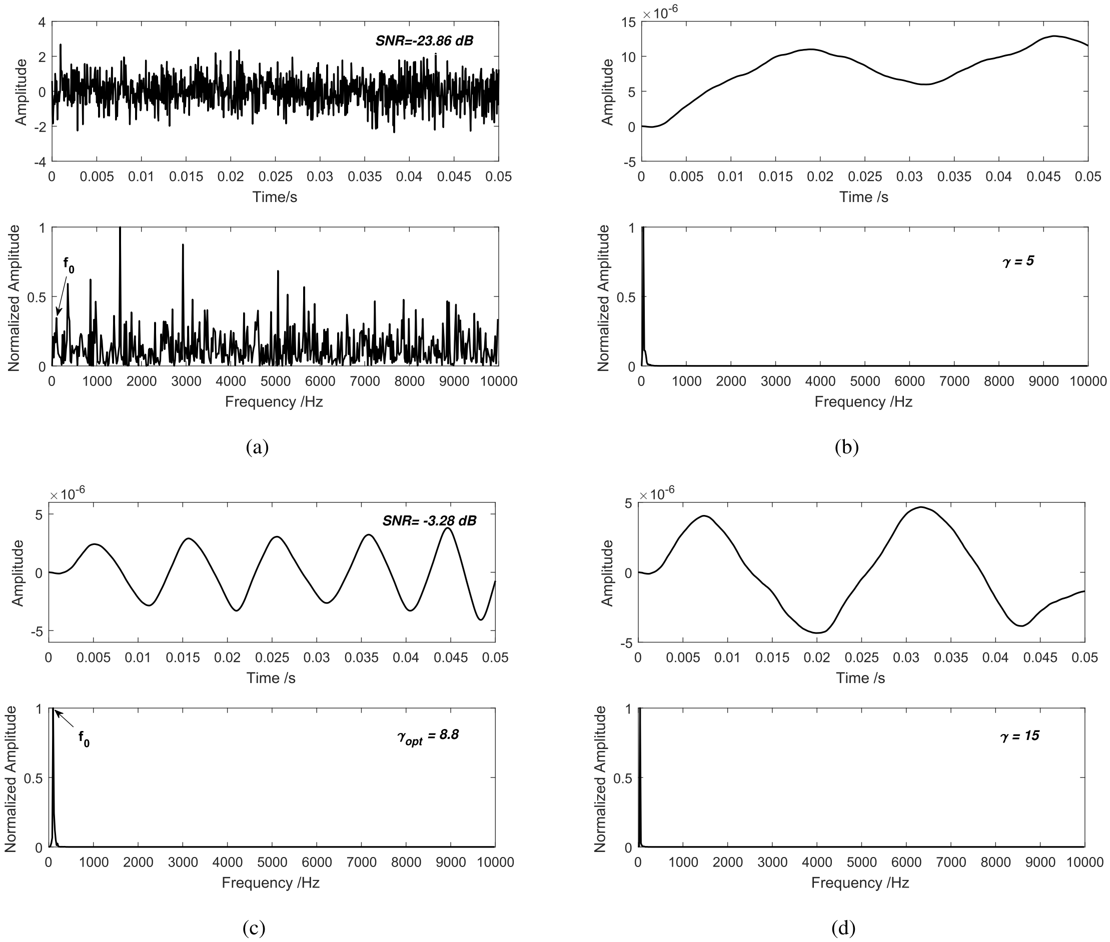

FIGURE 3. A comparison of SMSR and FMSR with (fixed $f = 100$Hz, $A = 0.1$, $D. = 1.2$) (a) The input waveform; (b) SMSR output waveform and its frequency spectrum with $\gamma = 5$. (c) SMSR optimal output waveform and its frequency spectrum with $\gamma_{opt} = 8.8$. (d) SMSR output waveform and its frequency spectrum with $\gamma = 15$.

B. DAMPING FACTOR ANALYSIS

Intuitively, the damping factor γ plays a critical role in determining the matched system parameters for desired optimal output. Therefore, the optimal damping factor γ_{opt} corresponding to the matched output with different driving frequencies and noise intensities are firstly analyzed in the framework of the proposed SMSR method. The tested signals are sinusoids with random AWGN, of which the signal amplitude and the data length are fixed with $A = 0.1$ and $N = 1000$, respectively. The tuning range and tuning step of damping factor are loaded with $[\gamma_{start}, \gamma_{end}] = [0.1, 300]$ and $\gamma_{step} = 0.1$, respectively. As shown in Fig.3, a simulation of SMSR with different damping factors is illustrated to verify the effectiveness of tuning. The selected input is a noisy signal (-23.86 dB) as show in Fig.3(a), of which the periodic signal waveform is totally immersed in background noise and the spectral spike at $f_0 = 100Hz$ can be hardly found in frequency domain, either. Fig.3(b)-(d) have shown the SMSR output waveform and its corresponding frequency spectrum for different damping factors, it is clear to see the noise interference of matched output with $\gamma_{opt} = 8.8$ (in Fig.3(c)) is almost wiped out in achieving a 20dB enhancement of SNR. Nevertheless, the unmatched output with $\gamma = 5$ (in Fig.3(b)) and $\gamma = 15$ (in Fig.3(d)) exhibit a Lorentzian property that the energy of output is more tended to be transferred to the low-frequency regions.

To further evaluate the statistical characteristic of optimal damping factors, 2000 independent realizations are conducted with varied driving frequencies and noise intensities, respectively. Fig.4 shows the frequency response of optimal damping factors with varied f_0 from 1Hz to 10kHz in fixing noise intensity $D = 0.8$. It can be seen that the values of optimal damping factors present an increasing tendency with driving frequencies, of which the distribution range of damping factors can be verified that is proportional to the driving frequency f_0. These results are in accordance with the deduced restriction interval of equation (14) by Lyapunov's stability analysis, and can be a principle for initializing the tuning range for different applications. The noise response of optimal damping factors is illustrated in Fig.5 with $f_0 = 100Hz$, of which the values of optimal damping factors are generally distributed in a certain range between 5 to 40.

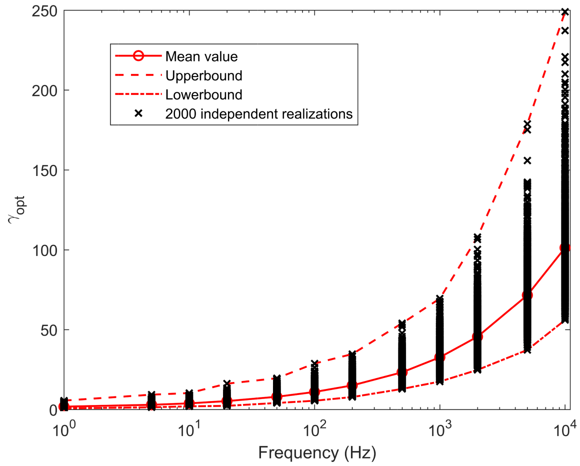

FIGURE 4. Frequency response of optimal damping factors with 2000 independent realizations (fixed $A = 0.1$, $D = 0.8$).

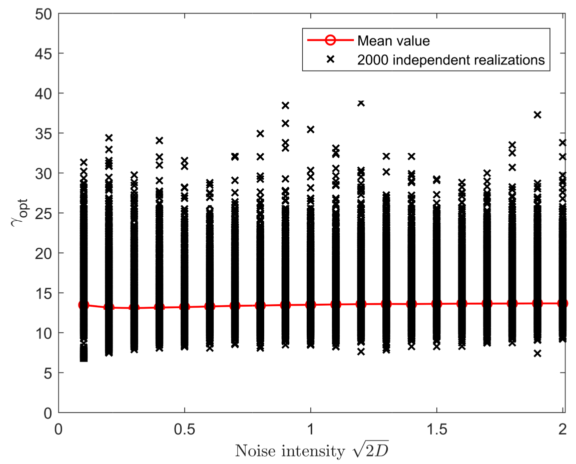

FIGURE 5. Noise response of optimal damping factors with 2000 independent realizations (fixed $A = 0.1$, $f_0 = 100Hz$).

The fluctuations are mainly caused by the random property of additive noise, for which the mean values of SNRI with varying noise intensity almost form a line. This indicates that the restriction interval for SMSR method is irrelevant to noise intensity as illustrated in equation (14), and the tuning interval can be initialized according to the being detected driving frequency.

C. DENOISING PERFORMANCE EVALUATION

As mentioned before, SR can be regarded as a specific kind of filter. In this subsection, the denoising performance of the proposed second-order matched stochastic resonance (SMSR) is evaluated in comparison with first-order matched stochastic (FMSR) [31]. The tested signal is a sinusoid with $A = 0.1$ and $f_0 = 100Hz$ as shown in Fig.6(a), in which the sampling frequency is set as $f_s = 200\, f_0$ with the data length $N = 1000$. The bistable potential parameters a and b are determined by equation(13) with a_{match} and b_{match}, and the tuning range and tuning step of damping factor

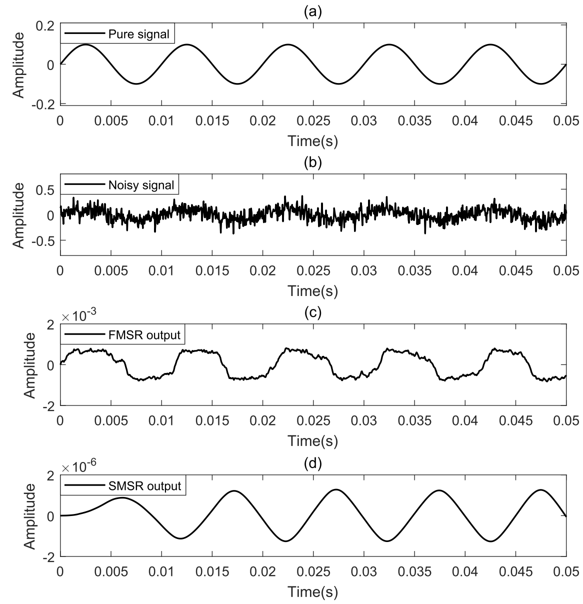

FIGURE 6. Filtering performance comparison: (a) pure signal; (b) input noisy signal; (c) FMSR output signal; (d) SMSR output signal at $\gamma_{opt} = 23.2$.

are loaded to $[\gamma_{start}, \gamma_{end}] = [5, 40]$ and $\gamma_{step} = 0.1$, respectively. To illustrate the basic properties of the proposed SMSR method, an AWGN with noise intensity $D = 0.2$ is injected to the pure signal as illustrated in Fig.6(b). Fig.6(c) displays the matched output of the FMSR method, for which the sinusoid is almost recovered from the noisy signal, while some noise interference can still be noticed. By employing the proposed SMSR method in this paper, the recovered signal is almost noise-free with a phase deviation[1] of π as demonstrated in Fig.6(d). In addition, phase portraits corresponding to Fig.6 are plotted in Fig.7 for a deeper observation of particle motion. The pure signal produces a deterministic elliptic trajectory as shown in Fig.7(a), while totally destroyed to

[1]Note in our simulation the phenomenon of phase deviation is steady that makes no difference to the utilization.

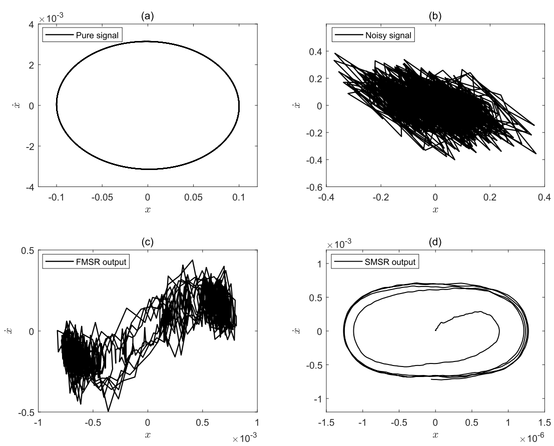

FIGURE 7. Phase portraits of particle trajectories corresponding to the signals illustrated in Fig.6.

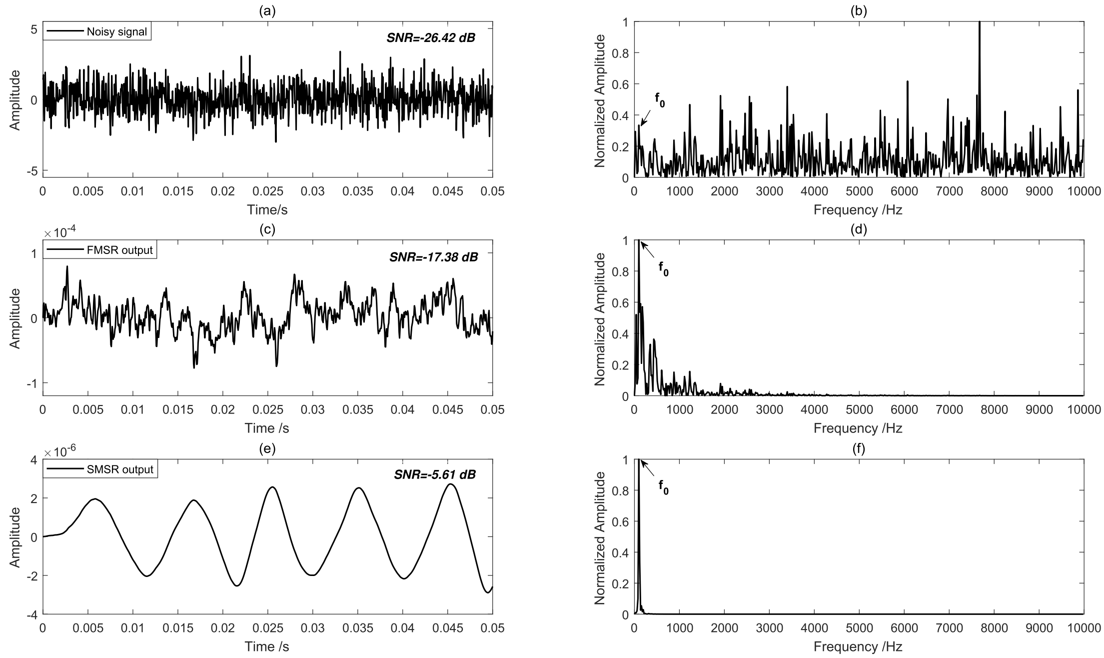

FIGURE 8. **A simulation of SMSR with different damping factors (fixed $f = 100$Hz, $A = 0.1$, $D = 1.2$) (a) waveform of input noisy signal, (b) spectrum of input signal, (c) FMSR output waveform with $\gamma_{opt} = 1.41$, (d)spectrum of FMSR output, (e) SMSR output waveform with $\gamma_{opt} = 10.8$, (f) spectrum of SMSR output.**

a state of chaotic with additive white Gaussian noise that illustrated in Fig.7(b). Fig.7(c) reflects a form of particle transition between two potential wells corresponding to FMSR, while the noise interference is still significant. By utilizing the proposed SMSR method, the particle trajectory behaves well-ordered that quickly evolve into an approximately elliptic trajectory as demonstrated in Fig.7(d). From the above analyses, it can be seen the proposed SMSR could achieve a better denoising performance in which more noise interference is wiped out.

To further evaluate the denoising performance of SMSR in comparison with FMSR under heavy noise background, an AWGN with noise intensity $D = 1.2$ is added. From Fig.8(a) and Fig.8(b), we can note that the periodic signal is completely submerged in background noise both in time and frequency domain. By utilizing the FMSR method as illustrated in Fig.8(c) and Fig.8(d), the periodic component of FMSR output is still immersed in noise in time domain, while the spectral spike at $f_0 = 100Hz$ can be found. From a view of the frequency spectrum, the FMSR method can be regarded as a conventional bandpass filter. The output waveform and corresponding frequency spectrum of the proposed SMSR method are demonstrated in Fig.8(e) and Fig.8(f). In comparing in the time domain, it performs apparently periodic that the noise interference is almost filtered. The spectral spike at $f_0 = 100Hz$ in frequency domain is very sharp that can be thought as processed by an extremely narrow bandpass filter. These results imply that the second-order SR model is quite beneficial to extract the periodic signal from the heavy background noise.

The frequency response and noise response of the proposed SMSR in comparison with FMSR are further analyzed to evaluate the performance in handling with different driving frequencies and noise levels. To evaluate the performance for arbitrary periodic inputs, the averaging SNRI (SNRI_{mean}) of FMSR and proposed SMSR method with varied driving frequencies f_0 from 1Hz to 10kHz are analyzed, and every data point is obtained by averaging 2000 independent realizations. The results are plotted in Fig.9, in which the SNRI_{mean} curve of the SMSR method shows a distinct superior performance

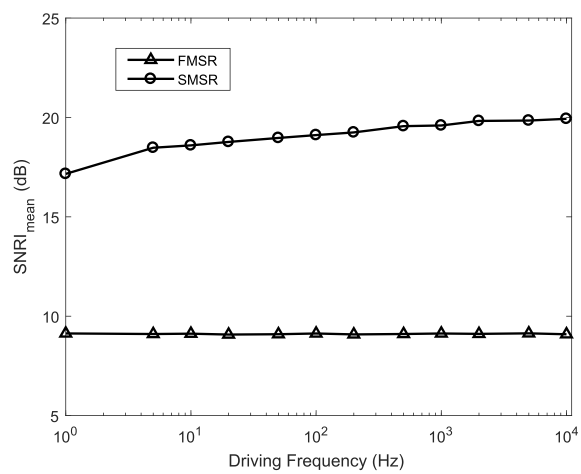

FIGURE 9. **SNRI comparison between FMSR method and the proposed SMSR method with varying driving frequencies with 2000 independent realizations (fixed $D = 0.8$).**

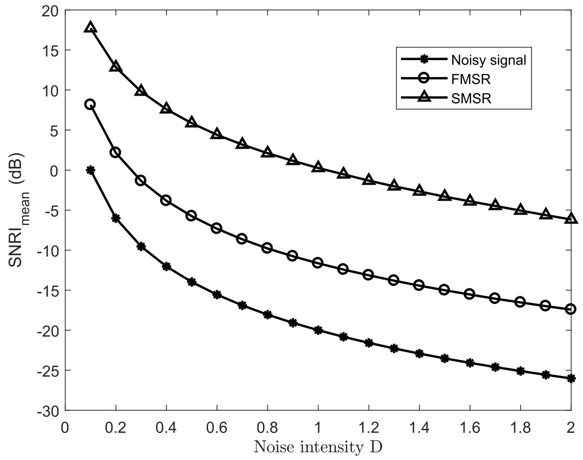

FIGURE 10. SNRI comparison between FMSR method and the proposed SMSR method with varied noise intensities with 2000 independent realizations (fixed $f_0 = 1kHz$).

in comparison with FMSR method. For the proposed SMSR method, the curve shows a gradually increasing tendency to the driving frequency f_0, while for FMSR it seems more consistent. This is because the normalized scale transformation of FMSR is totally equivalent to a system with potential parameters of $a = 1$ and $b = 1$, and as a result, the restricted interval of γ is determinate that can not be over $2\sqrt{2}$. Nevertheless, the restricted interval of γ for SMSR method is proportional to driving frequency f_0 as deduced and verified before. This means for SMSR method, a smaller frequency signal corresponds to a smaller tuning range, thus the output performance for a low frequency (smaller than 1Hz) input signal would tend to FMSR method or worse. The noise response of the proposed SMSR in comparison with FMSR is plotted in Fig.10 to evaluate the anti-noise performance in handling different levels of noisy signals. The tested signals are sinusoids with fixed amplitude and frequency as $A = 0.1$, $f_0 = 1kHz$, and the noise intensity D is altered from 0.1 to 2 with a 0.1 varying step. Obviously, the proposed SMSR method shows distinct superiority in comparison with FMSR as its SNRI_{mean} curve is highly above that of the FMSR method. The noise response curve exhibits a gradual upward trend with the increasing noise intensity, which is for the sake of limited enhancement performance for higher SNR input signal. These results imply that the proposed SMSR is quite beneficial to extract the periodic signal from the heavy background noise. Fig.11 demonstrates a comparison of FMSR and SMSR output waveform and the corresponding frequency spectrum with different driving frequencies. For input driving frequency $f_0 = 0.1Hz$, the output waveform and the corresponding frequency spectrum of FMSR and

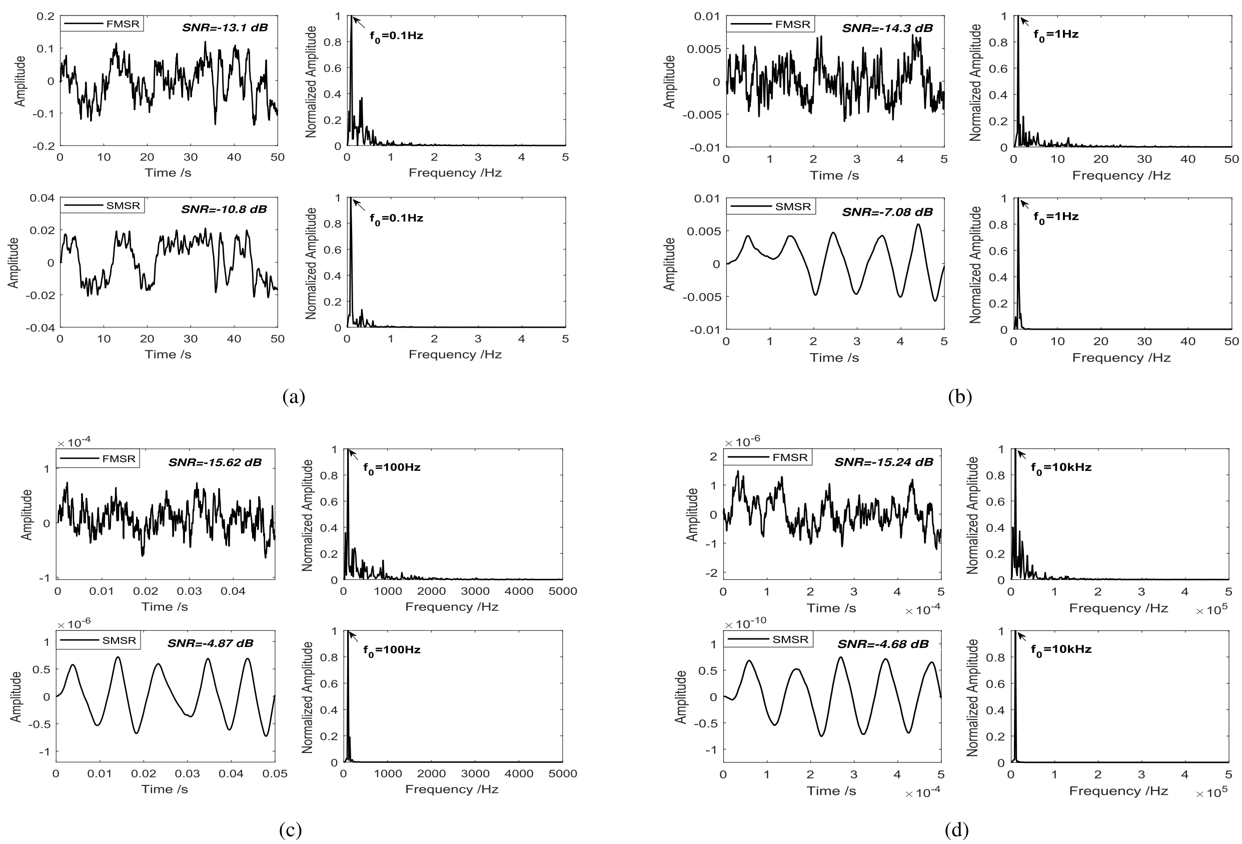

FIGURE 11. A comparison of SMSR and FMSR output waveform and corresponding frequency spectrum with different driving frequencies (a) 0.1Hz, (b) 1Hz, (c) 100Hz, (d) 10kHz (fixed $A = 0.1$, $D = 0.8$).

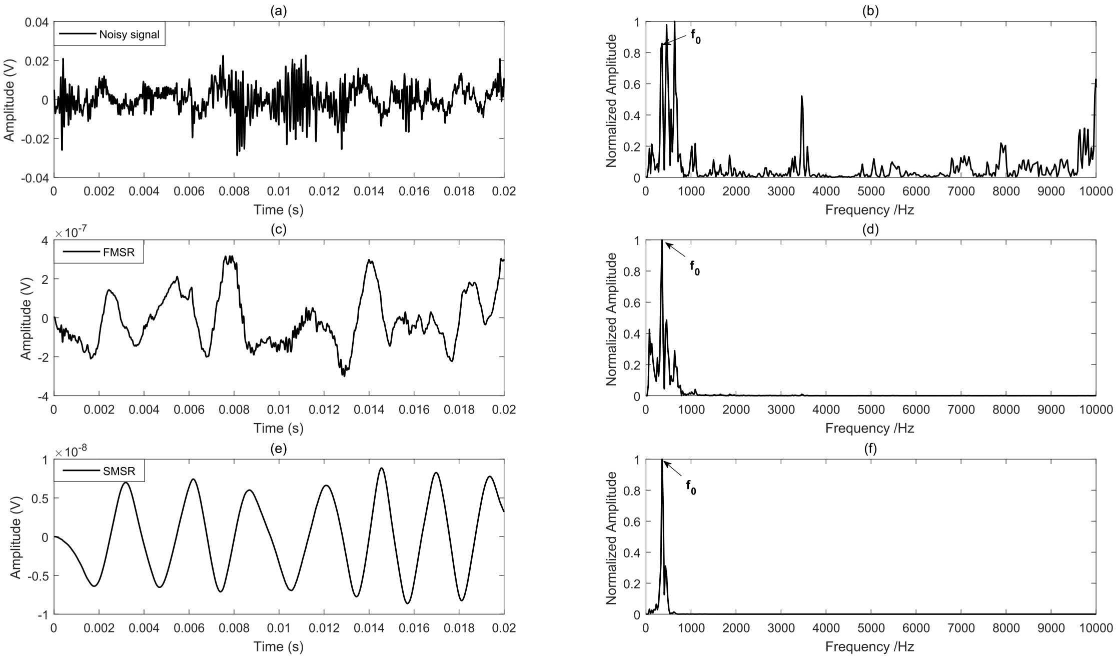

FIGURE 12. Analyzed result for ship auxiliary engine line-spectrum signature (a) waveform of received original ship radiated acoustic signal, (b) spectrum of original ship radiated acoustic signal, (c) FMSR output waveform with $\gamma_{opt} = 1.21$, (d) spectrum of FMSR output, (e) SMSR output waveform with $\gamma_{opt} = 45.3$, (f) spectrum of SMSR output.

SMSR method are close with just 2.3 dB enhancement as is shown in Fig.11(a). After gradually increasing the driving frequencies, the output performance of SMSR method indicates superiority to FMSR method. This means the proposed SMSR method is more suitable for detecting high-frequency signals, which can meet the need of practical engineering applications for the majority of research fields.

IV. APPLICATION VERIFICATION

To validate the effectiveness and efficiency of the proposed SMSR method in practical passive sonar detection application, a set of acoustic data by a moving ship is adopted to analyze. The radiated noise was received by a hydrophone with sampling frequency $f_s = 100kHz$.

Here, the auxiliary engine discrete spectral signature is being detected with original received ship radiated acoustic signal, which is a narrow band periodic signal with its frequency $f_0 = 356.2Hz$. To verify the performance of SMSR, a 20 milliseconds fragment of data is utilized with sampling points $N = 2000$. The waveform and its low frequency zone frequency spectrum of original signal is shown in Fig.(12)(a) and Fig.(12)(b), of which the spectral signature can be pointed out in the frequency spectrum with two strong interference frequencies. By applying the FMSR method, the output and its corresponding low frequency zone spectrum is provided in Fig.(12)(c) and Fig.(12)(d). An indistinct periodic in the time domain can be seen, and the spectral spike at f_0 in the frequency spectrum can be detected easily with the noise component being suppressed. Finally, results of the proposed SMSR method are provided in Fig.(12)(e) and Fig.(12)(f), where the waveform is well arranged with good periodicity and the spectral spike at f_0 in power spectrum is more clear with little noise components. Although the noise can still be found in the power spectrum, such a result is excellent in comparing with FMSR method and beneficial to ship radiated line-spectrum detection.

Beside the performance comparison, the time consuming is recorded in Matlab R2017a on the platform configured with the following parameters: Intel i5, 3.2-GHz Quad Core processor, 8-GB memory, 64-bit-win10 operating system. The tuning range and tuning step of damping factor for SMSR are loaded with $[\gamma_{start}, \gamma_{end}] = [10, 70]$ (reference Fig.4 with $f_0 = 356.2Hz$) and $\gamma_{step} = 0.1$, which totally searching 600 steps. For FMSR method, the tuning range and tuning step are initialized with $[\gamma_{start}, \gamma_{end}] = [0.8, 3]$ and $\gamma_{step} = 0.01$, which totally searching 220 steps. The computational time for FMSR and SMSR is 0.389s and 2.705s, respectively. It can be seen that the computational cost of SMSR method is about 7 times that of FMSR method which caused by the different searching steps of damping factor and the computation complexity of second order system is approximate 2.5 times that of first order system by applying the corresponding RK4 methods. Note that the computational cost of SMSR method is proportional to driving frequency f_0, which can be utilized efficiently in determining the searching ranges and intervals with low computational costs for different frequency band signals.

V. CONCLUSION AND DISCUSSION

This paper proposes an SMSR method for improving the performance of weak period signal detection. In combining noise optimization and frequency synchronization of duffing system with normalized scale transformation, a second-order parameter matched relationship is deduced and the corresponding signal processing strategy is given that could detect arbitrary high frequency signals subjected to heavy noise interference. Numerical analysis and application verification are conducted in comparison with FMSR method, which indicates that the proposed SMSR method surpasses the FMSR method in achieving a superior performance.

Although the results of SMSR are inspired in weak signal detection area, the utilization in practical is still limited as of input-output SNRI measurement index with matched output tuning generally need prior knowledge of signal frequency (e.g. passive sonar detection, the frequency information of line-spectrum feature is generally prior unknown with time-varied operating condition of vessels). It is still an open problem, which can be solved by applying other measurement index such as: mutual information between input and output signals, highest spectral peak location, kurtosis index, root mean square error, synthetic index with the fusion of multi-measurement indexes, and etc. For the future, we anticipate the proposed method can be used as a potential technique for a variety of research fields.

REFERENCES

[1] R. Benzi, A. Sutera, and A. Vulpiani, "The mechanism of stochastic resonance," *J. Phys. A, Math. Gen.*, vol. 14, no. 11, pp. L453–L457, 1981.
[2] B. McNamara and K. Wiesenfeld, "Theory of stochastic resonance," *Phys. Rev. A, Gen. Phys.*, vol. 39, no. 9, pp. 4854–4869, 1989.
[3] L. Gammaitoni and P. Hänggi, P. Jung, and F. Marchesoni, "Stochastic resonance," *Rev. Mod. Phys.*, vol. 70, no. 1, pp. 223–287, 1998.
[4] F. Chapeau-Blondeau, "Input-output gains for signal in noise in stochastic resonance," *Phys. Lett. A*, vol. 232, nos. 1–2, pp. 41–48, 1997.
[5] Z. Gingl, P. Makra, and R. Vajtai, "High signal-to-noise ratio gain by stochastic resonance in a double well," *Fluctuation Noise Lett.*, vol. 1, no. 3, pp. L181–L188, 2001.
[6] P. Makra, Z. Gingl, and T. Fülei, "Signal-to-noise ratio gain in stochastic resonators driven by coloured noises," *Phys. Lett. A*, vol. 317, nos. 3–4, pp. 228–232, 2003.
[7] V. Galdi, V. Pierro, and I. M. Pinto, "Evaluation of stochastic-resonance-based detectors of weak harmonic signals in additive white Gaussian noise," *Phys. Rev. E, Stat. Phys. Plasmas Fluids Relat. Interdiscip. Top.*, vol. 57, no. 6, pp. 6470–6479, 1998.
[8] S. Kay, "Can detectability be improved by adding noise?" *IEEE Signal Process. Lett.*, vol. 7, no. 1, pp. 8–10, Jan. 2000.
[9] S. Zozor and P.-O. Amblard, "On the use of stochastic resonance in sine detection," *Signal Process.*, vol. 82, no. 3, pp. 353–367, 2002.
[10] H. Chen, P. K. Varshney, S. M. Kay, and J. H. Michels, "Theory of the stochastic resonance effect in signal detection: Part I—Fixed detectors," *IEEE Trans. Signal Process.*, vol. 55, no. 7, pp. 3172–3184, Jul. 2007.
[11] H. Chen and P. K. Varshney, "Theory of the stochastic resonance effect in signal detection: Part II—Variable detectors," *IEEE Trans. Signal Process.*, vol. 56, no. 10, pp. 5031–5041, Oct. 2008.
[12] S. Zozor and P. O. Amblard, "Stochastic resonance in locally optimal detectors," *IEEE Trans. Signal Process.*, vol. 51, no. 12, pp. 3177–3181, Dec. 2003.
[13] V. N. Hari, G. V. Anand, A. B. Premkumar, and A. S. Madhukumar, "Design and performance analysis of a signal detector based on suprathreshold stochastic resonance," *Signal Process.*, vol. 92, no. 7, pp. 1745–1757, 2012.
[14] F. Duan, F. Chapeau-Blondeau, and D. Abbott, "Non-Gaussian noise benefits for coherent detection of narrowband weak signal," *Phys. Lett. A*, vol. 378, nos. 26–27, pp. 1820–1824, 2014.
[15] X. Zhang, J. Yan, and F. Duan, "Comparison of bistable systems and matched filters in non-Gaussian noise," *Fluctuation Noise Lett.*, vol. 15, no. 1, p. 1650003, 2016.
[16] B. Xu, F. Duan, R. Bao, and J. Li, "Stochastic resonance with tuning system parameters: The application of bistable systems in signal processing," *Chaos, Solitons Fractals*, vol. 13, no. 4, pp. 633–644, 2002.
[17] H. Niaoqing, M. Chen, and W. Xisen, "The application of stochastic resonance theory for early detecting rub-impact fault of rotor system," *Mech. Syst. Signal Process.*, vol. 17, no. 4, pp. 883–895, 2001.
[18] Y. G. Leng, Y. S. Leng, T. Y. Wang, and Y. Guo, "Numerical analysis and engineering application of large parameter stochastic resonance," *J. Sound Vib.*, vol. 292, nos. 3–5, pp. 788–801, 2006.
[19] L. Qiang, W. Taiyong, L. Yonggang, W. Wei, and W. Guofeng, "Engineering signal processing based on adaptive step-changed stochastic resonance," *Mech. Syst. Signal Process.*, vol. 21, no. 5, pp. 2267–2279, 2007.
[20] J. Tan *et al.*, "Study of frequency-shifted and re-scaling stochastic resonance and its application to fault diagnosis," *Mech. Syst. Signal Process.*, vol. 23, no. 3, pp. 811–822, 2009.
[21] Q. He, J. Wang, Y. Liu, D. Dai, and F. Kong, "Multiscale noise tuning of stochastic resonance for enhanced fault diagnosis in rotating machines," *Mech. Syst. Signal Process.*, vol. 28, no. 2, pp. 443–457, 2012.
[22] J. Wang, X. Ren, S. Zhang, D. Zhang, H. Li, and S. Li, "Adaptive bistable stochastic resonance aided spectrum sensing," *IEEE Trans. Wireless Commun.*, vol. 13, no. 7, pp. 4014–4024, Jul. 2014.
[23] Y.-G. Leng, T.-Y. Wang, Y. Guo, Y.-G. Xu, and S.-B. Fan, "Engineering signal processing based on bistable stochastic resonance," *Mech. Syst. Signal Process.*, vol. 21, no. 1, pp. 138–150, 2007.
[24] Y.-G. Leng, "Mechanism of parameter-adjusted stochastic resonance based on Kramers rate," *Acta Phys. Sinica*, vol. 58, no. 8, pp. 5196–5200, 2009.
[25] S. Lu, Q. He, and F. Kong, "Effects of underdamped step-varying second-order stochastic resonance for weak signal detection," *Digital Signal Process.*, vol. 36, pp. 93–103, Jan. 2015.
[26] Z.-H. Lai and Y.-G. Leng, "Generalized parameter-adjusted stochastic resonance of duffing oscillator and its application to weak-signal detection," *Sensors*, vol. 15, no. 9, pp. 21327–21349, 2015.
[27] Z.-H. Lai and Y.-G. Leng, "Weak-signal detection based on the stochastic resonance of bistable duffing oscillator and its application in incipient fault diagnosis," *Mech. Syst. Signal Process.*, vol. 81, pp. 60–74, Dec. 2016.
[28] X. Liu, J. Yang, H. Liu, G. Cheng, X. Chen, and D. Xu, "Optimizing the adaptive stochastic resonance and its application in fault diagnosis," *Fluctuation Noise Lett.*, vol. 14, no. 4, p. 1550038, 2015.
[29] Y. Qin, Y. Tao, Y. He, and B. Tang, "Adaptive bistable stochastic resonance and its application in mechanical fault feature extraction," *J. Sound Vib.*, vol. 333, no. 26, pp. 7386–7400, 2014.
[30] Z. Qiao, Y. Lei, J. Lin, and F. Jia, "An adaptive unsaturated bistable stochastic resonance method and its application in mechanical fault diagnosis," *Mech. Syst. Signal Process.*, vol. 84, pp. 731–746, Feb. 2017.
[31] H. Dong, H. Wang, and X. Shen, "Parameter matched stochastic resonance enhanced passive sonar detection," *J. Acoustic Soc. Amer.*, to be published.
[32] J. Li, X. Chen, Z. Du, Z. Fang, and Z. He, "A new noise-controlled second-order enhanced stochastic resonance method with its application in wind turbine drivetrain fault diagnosis," *Renew. Energy*, vol. 60, pp. 7–19, Dec. 2013.
[33] Q. Ma, D. Huang, and J. Yang, "Adaptive stochastic resonance in second-order system with general scale transformation for weak feature extraction and its application in bearing fault diagnosis," *Fluctuation Noise Lett.*, vol. 17, no. 1, p. 1850009, 2018.
[34] I. Kovacic and M. J. Brennan, *The Duffing Equation: Nonlinear Oscillators and Their Behaviour*. Chichester, U.K.: Wiley, 2011.
[35] S. M. Kay, *Fundamentals of Statistical Signal Processing: Estimation Theory*, vol. 1. Englewood Cliffs, NJ, USA: Prentice-Hall, 1993.

HAITAO DONG received the B.S. and M.S. degrees in electrical engineering from the School of Marine Science and Technology, Northwestern Polytechnical University, Xi'an, China, in 2011 and 2014, respectively, where he is currently pursuing the Ph.D. degree with the Key Laboratory of Ocean Acoustics and Sensing. His research interests lie in the areas of underwater passive sonar weak signal processing, stochastic resonance-based nonlinear filter, and ship radiated noise signature extraction.

HAIYAN WANG received the B.S., M.S., and Ph.D. degrees from the School of Marine Science and Technology, Northwestern Polytechnical University (NPU), Xi'an, China, in 1987, 1990, and 2004, respectively. He has been a Faculty Member of NPU since 1990 and a Professor since 2004. He teaches and conducts research at NPU in the areas of signal and information processing, electronic engineering, and tracking and locating of maneuvering targets. His general research interests include modern signal processing, array signal processing, underwater acoustic communications, tracking and locating of maneuvering targets, and data mining technique and its application.

XIAOHONG SHEN received the B.S., M.S., and Ph.D. degrees in electrical engineering from the School of Marine Science and Technology, Northwestern Polytechnical University (NPU), Xi'an, China, in 1987, 1998, and 2008, respectively. She has been a Faculty Member of NPU since 1987 and a Professor since 2010. She teaches and conducts research at NPU in the areas of signal and information processing, communication and information system, and electronic engineering. Her general research interests include underwater acoustic communication and networking, modern signal processing, information fusion, and tracking and locating of maneuvering targets.

ZHE JIANG received the B.S. degree in electrical engineering and information science from Xidian University, Xi'an, China, in 2006, and the M.S. and Ph.D. degrees from the School of Marine Science and Technology, Northwestern Polytechnical University (NPU), Xi'an, in 2008 and 2012, respectively. He joined the School of Marine Science and Technology, NPU, in 2013. His research interests lie in the areas of communications and signal processing, including the channel estimation and equalization, multicarrier communications, space–time coding, adaptive modulation, and underwater acoustic communications.